Thermal Transitions in Hydrogels of Poly(ethyl acrylate)/ Poly(hydroxyethyl acrylate) Interpenetrating Networks

J. Rault,† A. Lucas,† R. Neffati,† and M. Monleón Pradas*,‡

Laboratoire de Physique des Solides, Université de Paris-Sud, Bât. 510, F-91405 Orsay, France, and Departamento de Termodinámica Aplicada, Universidad Politécnica, P. O. Box 22012, E-46071 Valencia, Spain

Received March 12, 1997; Revised Manuscript Received September 16, 1997⊗

ABSTRACT: The thermal transitions observed in hydrogels based on interpenetrating networks of poly(ethyl acrylate) and poly(hydroxyethyl acrylate) are explained in a simple thermodynamic framework based on the phase diagram that avoids making use of the hypothesis of different "kinds" of water present in the hydrogel. The features that can be explained on its basis include the melting temperature depression of water, the occurrence of crystallization on heating (even when it was absent upon cooling), and the existence of an amount of noncrystallizable water. Three water concentration regimes can be predicted to exist, which give rise to qualitatively different kinds of thermograms.

1. Introduction

Polymer hydrogels have a great interest for pharmaceutical and medical applications. Their biocompatibility and water permeation properties lie at the base of these applications. However, many of their potential uses are hindered by their low mechanical strength. New families of polymers have been developed, seeking to improve the mechanical behavior of the corresponding hydrogels. Many efforts are directed toward polymers with microphase-separated morphologies, such as block copolymers, in which hydrophobic and hydrophilic domains alternate.[1] These multidomain structures seem to favor blood compatibility and possess improved mechanical properties. Another means to achieve such a goal is through interpenetrating polymer networks, IPNs.[2−4] In contrast to block copolymers, the phase morphology in these systems is stable against environmental changes because it is fixed by the cross-links. IPNs are indeed binary systems composed of two mixed polymers, each of which is individualy cross-linked;[5] even when both starting monomers are completely miscible, the thermodynamical stability of the monomer mixture is soon lost as the polymerization reaction proceeds, and phase separation sets in.[5,6] Nevertheless, factors such as the degree of cross-linking and the reaction kinetics can "freeze" the phase separation at an early stage, producing multicomponent polymer systems with more or less fine or coarse-grained micromorphologies.[6]

If one of the IPN components is hydrophilic, the IPN can form a polymer hydrogel when water is absorbed. The state of water and its influence on the hydrogel's properties thus become of primary importance. The complicated appearance of experimental heating and cooling thermograms in these materials has led to interpretations that often diverge. From these thermograms water has been inferred to exist in different states inside a hydrogel, such as a "bound" and a "free" state;[7−12] a continuum of intermediate states is also invoked sometimes.[7,11] The relative proportions of these states are thought to influence the hydrogel's mechanical properties.[8] On the other hand, partial heat capacity studies of water in hydrogels[12−15] reveal no such difference and, indeed, the existence of these different "kinds" of water has been explicitly challenged by giving alternative explanations of the shape of the thermograms.[13,14,16−20]

In this paper we study the thermal behavior of an IPN-based hydrogel and develop a general framework for the interpretation of thermal transitions in polymer hydrogels. In its scheme this model was advanced in ref 18−20; here it is explained in detail and extended to take into account the influence of the undercooling effects. These effects turn out to have a significant influence on the form of the measurable thermograms. Our system, based on poly(hydroxyethyl acrylate), has a lower glass transition temperature[21,22,15] than poly(hydroxyethyl methacrylate), which is the most frequently studied hydrogel. This circumstance greatly facilitates the study, as all relevant transitions take place under ambient temperature.

2. A Simple Model for the Interpretation of Thermal Transitions in Polymer Hydrogels

A polymer hydrogel is a mixture of two molecular species. Let us call m_0, m_w, and $m = m_0 + m_w$ the masses of, respectively, the dry polymer, water, and the hydrogel and $c = m_w/m$ the weight fraction of water in the hydrogel. We assume that in its rubbery state the hydrogel can be considered homogeneous and thus it constitutes a thermodynamical phase. Further, we suppose that no liquid−liquid phase separation occurs (perfect miscibility in the liquid state) and that only the solvent (water) can crystallize. Standard thermodynamics of binary systems then predicts that the melting temperature of the solvent will experience a decrease, the so-called cryoscopic depression, with respect to its pure-component melting temperature. For ideal mixtures this relationship reduces to the classical law of Raoult,[23] whereas for polymer/water systems the dependence may be deduced from the Flory−Huggins theory,[24,25] as explained in ref 19. The melting temperature T_m is thus a function of the mixture composition, $T_m = T_m(c)$, giving rise to the so-called *liquidus* curve in a state diagram (curve T_m on Figure 1a). In this paragraph we assume, for simplicity, that the crystallization temperature upon cooling, T_c, coincides with the melting temperature upon heating, T_m, and that both are equal to the equilibrium phase transition

* Corresponding author.
† Université de Paris-Sud.
‡ Universidad Politécnica.
⊗ Abstract published in *Advance ACS Abstracts,* December 1, 1997.

S0024-9297(97)00344-6 CCC: $14.00

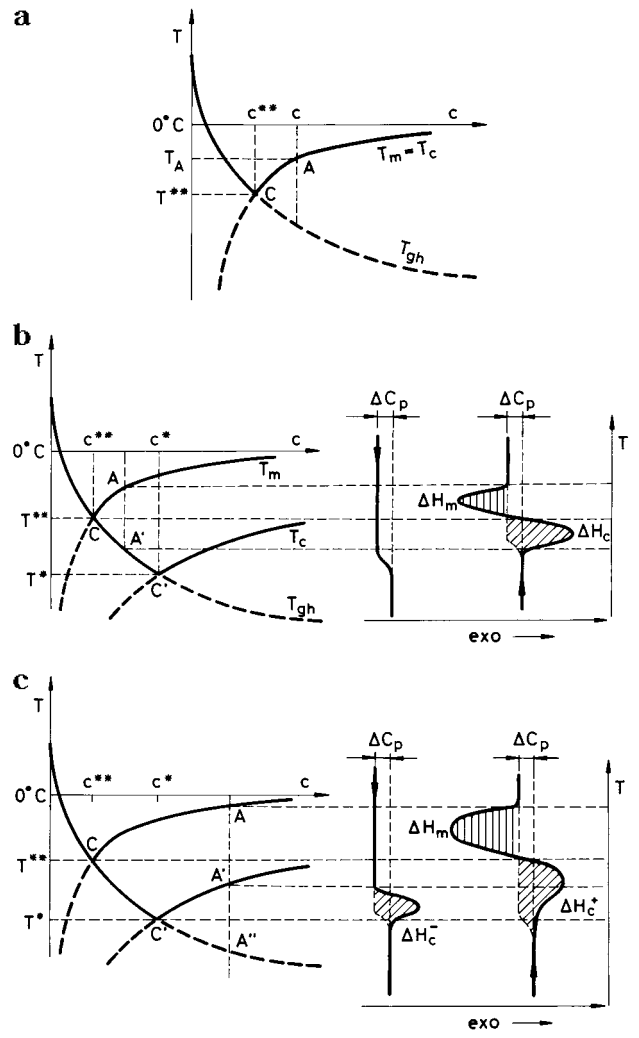

Figure 1. Transitions diagram of a polymer hydrogel: (a) without undercooling effects; (b) and (c) taking into account the undercooling of water crystallization. Expected shapes of the cooling and heating thermograms are drawn in (b) and (c). The diagrams show the dependence on water concentration of the (equilibrium) melting temperature T_m, the crystallization temperature T_c, and the hydrogel's glass transition temperature, T_{gh}.

temperature. In the next paragraph we analyze the effects of undercooling.

Without loss of validity, we neglect here the rate dependence of the value of the glass transition temperature of the xerogel T_{g0} and of the hydrogel T_{gh} since our considerations refer to experiments at one given, fixed constant rate. According to theories of mixtures,[26,27] T_{gh} depends on the hydrogel composition c and on both glass transition temperatures of the pure constituents, T_{g0}, T_{gw}; for given values of these last, the dependence $T_{gh} = T_{gh}(c)$ is monotonous, so T_{gh} will fall from T_{g0} for $c = 0$ to $T_{gw} = 134$ K (the T_g of water[28]) for $c = 1$ (curve T_{gh} on Figure 1a). The temperature−composition diagram of Figure 1a thus includes two curves, one defining the temperatures of an equilibrium phase change, $T_m(c)$, and the other one determining the temperatures of a kinetic nonequilibrium transition, $T_{gh}(c)$. Let us analyze on its basis the transitions experienced by a hydrogel upon cooling and heating at a given, constant rate.

The concentration of water c^{**} for which the glass transition temperature of the hydrogel and the phase change temperature of water become equal, $T_{gh}(c^{**}) = T_m(c^{**})$, delimits two composition intervals. If a hydrogel of composition c greater than c^{**} is cooled starting from ambient temperature, the single homogeneous phase will be stable until the temperature equals $T_m(c)$ (point A on Figure 1a). For lower temperatures the system is no longer stable as a homogeneous phase, and a pure solid water phase (water crystals) begins to separate. A two-phase system consisting of the hydrogel phase and the solid water phase results. When temperature is further decreased, the stability of the system can only be ensured if water migrates from the mixed (hydrogel) phase to grow the pure water phase, the hydrogel phase thus becoming poorer in water. The representative point of the hydrogel phase follows the arc AC on the liquidus curve in Figure 1a as the temperature falls from T_A to $T^{**} = T_m(c^{**})$; *i.e.*, the water concentration in the remaining amorphous hydrogel phase decreases and reaches the value c^{**} at T^{**}. At T^{**} the hydrogel phase experiences its glass transition: $T^{**} = T_{gh}(c^{**})$. The dramatic loss of mobility of the hydrogel's kinetic units results in a corresponding increase of viscosity of the phase. If this increase of viscosity is enough to impede the migration of the water molecules (as it will turn out experimentally to be the case), then the solid water phase can no longer grow at the expense of the hydrogel phase, and both phases become frozen with the amounts and compositions corresponding to these conditions. At any temperature lower than T^{**}, then, the system consists of a dispersed water solid phase and a vitreous homogeneous mixture of composition c^{**} and glass transition temperature T^{**}. Since the equilibrium composition of the hydrogel at that temperature would be that of its representative point on the *liquidus* curve instead of c^{**}, the system is at these temperatures in a state of "constrained", or metastable, equilibrium, from both the physical point of view (it is a glass) and the chemical point of view (since also the chemical composition differs from equilibrium). Notice that the same final state of the system (except for the total amounts of the phases) would be reached starting from any concentration higher than c^{**}. Thus, for $c > c^{**}$ the effective glass transition temperature of the hydrogel is independent of c and equal to T^{**}. This has been called the "T_g-regulation effect" in ref 18. An amount of water equal to mc^{**} can in no way be crystallized, and can thus be called "noncrystallizable water". Notice, however, that the existence of this noncrystallizable water is derived from purely thermodynamic considerations and makes no recourse to a postulated strong binding of some certain fraction of the water molecules to the polymer chains.

Heating of the previously frozen sample will induce no transition until the temperature T^{**} is reached; at this temperature both ice begins to melt (since $T^{**} = T_m(c^{**})$) and the glassy mixture will become rubbery (since $T^{**} = T_{gh}(c^{**})$). The liquid water originated in this way will mix with the hydrogel phase, whose representative point will now follow the path CA as the temperature increases until the original concentration is reached again.

If the starting water concentration in the hydrogel were $c < c^{**}$, the homogeneous phase would traverse at $T_{gh}(c) > T_m(c)$ its glass transition, before any crystallization of water can take place, Figure 1a. One would simply observe the glass transition of an amorphous polymer−solvent system, but no trace of the first-order transition of water corresponding to ice formation. All water contained in the hydrogel is counted as "noncrystallizable", although its binding to the polymer mol-

ecules needs in no way to be postulated different from that of water molecules taking part in crystallization.

Effect of Undercooling of Water. The picture just described does not take into account the undercooling effects that occur upon lowering the temperature. Whereas the melting temperature of water T_m reasonably equals the equilibrium phase transition temperature, it is well-known that, upon cooling, water does not crystallize until it reaches a temperature T_c that is significantly lower than T_m. Supercooling of 10−20 deg is often observed in pure water even for cooling rates as low as 0.2 deg/min. This is due to the fact that crystallization needs the occurrence of two processes, the formation of crystal *nuclei* (germs) on the one hand and their growth on the other. From a thermodynamical point of view this growth is associated with an increase in free energy due to the formation of the interface.[29,30] Only after a finite degree of undercooling can this increase be overweighed by the decrease in free energy associated with the growth of the new bulk phase. Further growth of the crystalline nuclei depends on the diffusion of the water molecules, which depends on the viscosity of their *milieu* and can thus be affected by the rate of change of temperature. Although a rate of cooling high enough can even prevent crystallization and result in glassy water,[28] for the experimentally common cooling rates from 1 to 20 deg/min that dependence is weak, and a $T_c = -21$ °C is obtained (curve of pure water in Figure 4). Upon cooling the hydrogel at a given rate, then, we expect to have a crystallization curve $T_c = T_c(c)$ different from the liquidus curve, with $T_c(c) < T_m(c)$ for each c (Figure 1b,c); this "hysteresis" has been often pointed out in hydrogels.[9,10,31]

The stable states of the hydrogel under given experimental conditions are determined by the *phase diagram* implied by the above considerations (Figure 1b,c): the curves T_{gh} and T_c determine the compositions of the stable states upon cooling, and the curves T_{gh} and T_m determine those of the stable states upon heating. These stable states might not always be attained, because of kinetic hindrances. Nevertheless, they always determine the direction of the evolution of the system.

Let us call c^* the concentration at which the crystallization temperature of water (at a fixed cooling rate) equals the glass transition temperature of the hydrogel: $T_c(c^*) = T_{gh}(c^*)$. Three concentration domains must be now distinguished.

(a) Concentration Regime $c < c^{**}$. For $c < c^{**}$ the discussion held above on the basis of Figure 1a retains its validity: for these compositions, no phase transition of water takes place, and all water is "noncrystallizable".

(b) Concentration Regime $c^{**} < c < c^*$. For water concentrations $c^{**} < c < c^*$ the hydrogel reaches $T_{gh}(c)$ before water can crystallize during cooling, $T_{gh}(c) > T_c(c)$, point A' in Figure 1b. Water could maybe crystallize in this temperature domain, but in times too long compared with the experimental time.[17] In common DSC rate experiments, then, water crystals are not able to form until T_c, but crystallization germs (*nuclei*) might appear during cooling in this temperature interval, their growth being impeded by the stability reasons given above and by the exponentially increasing viscosity of their surroundings. At $T_{A'}$ the system is frozen as a homogeneous phase as a consequence of its glass transition, and no further thermal transition can take place for $T < T_{A'}$. The thermogram of this process thus should show only the trace of the glass transition of the hydrogel (Figure 1b). Upon cooling below $T_{A'}$, nucleation of crystalline germs can occur, but growth of these germs is not possible.

Upon subsequent reheating, the system goes through its glass transition at $T_{A'}$; as T increases, the single-phase homogeneous state of the hydrogel with composition c will be unstable with respect to the two-phase state determined by the T_m curve on the phase diagram. This stable state consists of a crystal water phase plus a hydrogel phase of composition c_T^m on the liquidus curve at T, $T_m(c_T^m) = T$. Since $c_T^m < c$, this requires further separation of water from the hydrogel phase, and since the hydrogel is now above its glass transition temperature, micro-Brownian chain movements and decreased viscosity will allow the migration of water molecules necessary for the growth of the germs (some of them probably originated during the cooling stage), and water will crystallize as the temperature increases. This causes the hydrogel phase to become poorer in water. At any temperature T between $T_{A'}$ and T^{**} crystallization becomes again arrested when the water concentration of the hydrogel phase reaches the value c_T^g corresponding to T on the T_g curve; the more stable state with $c_T^m < c_T^g$ is thus kinetically impeded by the glass transition, and the representative point of the hydrogel phase follows the arc $A'C$ on the T_g curve in Figure 1b, until it reaches at temperature T^{**} the water concentration c^{**}. In this idealized picture, in which all changes demanded by the phase stability are supposed to take place actually (this requires low heating rates), crystallization of water would thus occur during heating from $T_{A'}$ to T^{**}, and the hydrogel phase would continuously change its composition and glass transition temperature in a way such that, if $T(t)$ is the experimental temperature at time t, then $T(t) = T_{gh}(c(t))$.

When the temperature T^{**} is passed, the phase equilibrium of solid water and the hydrogel phase of composition c^{**} becomes unstable with respect to an equilibrium of solid water and a hydrogel phase of composition $c^m > c^{**}$ on the T_m curve. Crystalline water thus begins to melt and diffuses into the hydrogel phase, increasing the latter's composition until the starting c. The representative point of the state of the hydrogel phase describes the path CA on the liquidus curve, and a melting endotherm appears on the heating thermogram (Figure 1b).

Summarizing, for hydrogel compositions in the interval $[c^{**}, c^*]$ no crystallization is to be expected during cooling, but a crystallization and subsequent melting must be expected upon heating. Still, an amount mc^{**} of water will not crystallize (whereas, if cooling alone were regarded, that amount would be mc^*). The trace of the process on the heating thermogram should thus include a first crystallization exothermal peak followed by the melting endotherm, and the baseline jump from the beginning to the end should correspond to the heat capacity jump at the glass transition found on the cooling thermogram (Figure 1b). A further specific prediction of the model refers to the width of the crystallization and melting peaks on the thermograms: since these transitions are predicted to take place between $T_{A'}$ and T_C and between T_C and T_A, their width should essentially coincide with these temperature intervals and be independent of the heating and cooling rates. This is in contrast to what would occur with the crystallization and melting of pure water, which result in peaks whose breadth tend to zero with the experi-

mental temperature rate.

(c) Concentration Regime $c > c^*$. The case $c > c^*$ is now easily compounded from those already discussed (Figure 1c). Upon cooling, water will crystallize from $T_{A'}$ till T^*, and the amount of ice formed will be m ($c - c^*$). The two-phase system becomes frozen at this temperature, with composition of the hydrogel phase c^* and T_g equal to T^*. For these water concentrations, then, the hydrogel's effective T_g on cooling is no longer given by $T_{A''} = T_{gh}(c)$ (Figure 1c), but is T^*, independent from c. Upon heating, water will again crystallize from T^* till T^{**}, while the hydrogel's T_g increases continuously in the same way, as explained in the foregoing paragraph. The amount of ice formed on heating is m ($c^* - c^{**}$), independent from the starting concentration. At T^{**} the amount of ice is maximum, and the water concentration in the remaining polymer−water phase is c^{**}. From that temperature on, water will melt and diffuse, thus increasing the hydrogel phase water concentration until the temperature $T_m(c)$, when the original situation is regained. The path described by the representative point of the hydrogel phase in the cycle will have been $A'C'CA$, and its trace on the cooling and heating thermograms will be as depicted in Figure 1c.

From the above discussion it follows that the interplay of thermodynamic equilibrium and nonequilibrium considerations determine a complex sequence of transitions in polymer hydrogels during constant rate cooling and heating thermal histories. These are reflected by very specific features of the experimental thermograms, which may serve to support the explanation here advanced of their origin. They include the existence of different quantities of noncrystallizable water upon cooling, mc^*, and upon heating, mc^{**}; the existence of three qualitatively different concentration regimes, characterized by the presence or absence of crystallization and melting during cooling and during heating; and the rate independence of the breadth of the first-order transition peaks.

3. Experimental Section

Monomer solutions of ethyl acrylate and hydroxyethyl acrylate were prepared, each containing a 2% weight of ethylene glycol dimethacrylate (cross-linking agent), EGDMA, and 0.13% benzoin (initiator). Polymerizations were carried out between glass plates under UV light for 24 h. Poly(ethyl acrylate) (PEA) was polymerized from the ethyl acrylate solution. Interpenetrating polymer networks (IPN) of PEA and poly(hydroxyethyl acrylate) (PHEA) were prepared by the sequential method.[5] The PEA network prepared as described above was swollen with the HEA monomer solution for 24 h, a swelling time which ensured that the network was swollen to equilibrium and that monomer had diffused homogeneously inside it. The swollen sample was then polymerized between glass plates as described.

The PEA homopolymer and the IPNs were rinsed in boiling ethanol for 24 h, and dried afterward under vacuum at 80 °C until their weight remained constant. The weight fraction of PHEA in the IPN was gravimetrically determined to be 0.754.

Samples for DSC were cut from the plates thus obtained. IPN samples were swollen in distilled water for different times so as to achieve hydrogel compositions c (mass of water/mass of swollen IPN) of 0.076, 0.164, 0.185, 0.200, 0.218, 0.250, 0.276, 0.316, and 0.346, which was the maximum water uptake of the IPN.

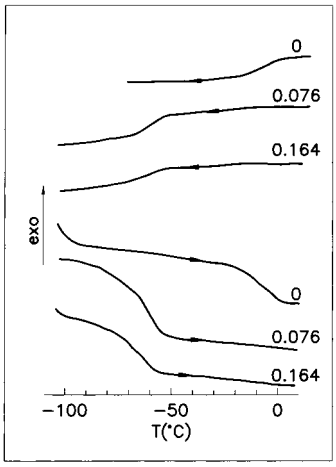

Figure 2. Cooling and heating thermograms of IPN samples with water concentration $c = 0$, 0.076, 0.164.

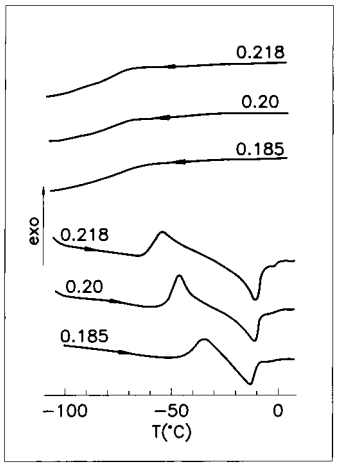

Figure 3. Cooling and heating thermograms of IPN samples with water concentration $c = 0.185$, 0.200, 0.218.

Water was carefully wiped off the samples' surfaces with absorbing paper, and each sample was immediately weighed and encapsulated in the DSC aluminum pans.

Differential scanning calorimetry (DSC) was performed in a Mettler TA 3000 apparatus, which gives as output the heat power (mW) communicated to the sample during the scan. Glass transition temperatures T_g and enthalpy increments are calculated by the apparatus software. The T_g values here reported correspond to the inflection point of the thermogram at the transition. All samples were subjected to the same thermal history, which consisted of a cooling scan from ambient temperature down to −110 °C, followed by a heating scan from that temperature up to 10 °C, both scans at a rate of 5 deg/min. Each sample was measured at least two times, and the results showed repeatability. The cooling-and-heating cycle was performed on an IPN hydrogel sample ($c = 0.346$) and on a pure bulk water sample at the rates of 1, 2, 5, and 10 K/min in order to assess the dependence of the width of the transition peaks on the temperature rate.

4. Results

Figures 2−4 show the cooling and heating thermograms of the swollen IPNs at different water concentrations. Samples with c up to 0.164 (Figure 2) show, on cooling and on heating a single transition, which corresponds to the glass transition of the hydrogel. The temperature of this transition is separated a couple of

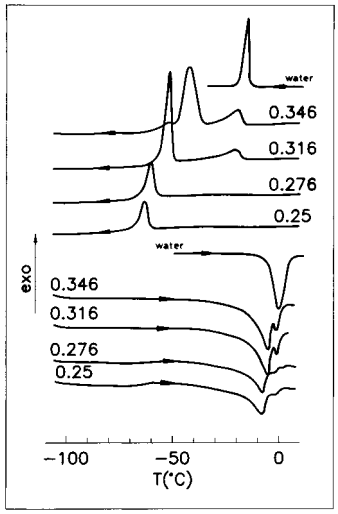

Figure 4. Cooling and heating thermograms of IPN samples with water concentration $c = 0.250$, 0.276, 0.316, 0.346 and of pure water.

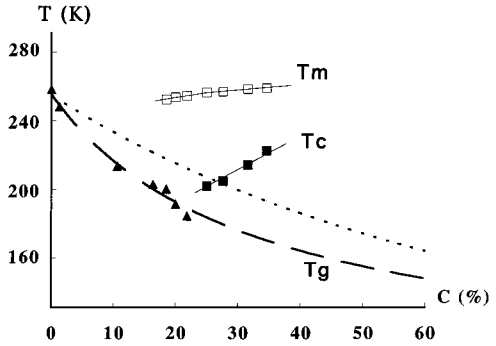

Figure 5. Experimental temperature-composition diagram for the IPN hydrogel: (▲) glass transition temperature of the hydrogel; (■) crystallization temperature of water on cooling; (□) melting temperature of water on heating; (···) glass transition temperature predicted by the Fox equation (1) for a homogeneous blend of two species having the T_g's of pure water and of the dry IPN; (−−−) glass transition temperature predicted by the Couchman−Karasz equation (2) for a homogeneous blend of two species having the T_g's and $\Delta c_p(T_g)$'s of pure water and of the dry IPN.

degrees in both scans, and in both of them T_g shifts toward lower temperatures as c increases. The cooling thermograms of samples with $c = 0.185$ up to $c = 0.218$ (Figure 3) show only the glass transition of the hydrogel. The heating thermograms are now more complex. The glass transition is again visible in the same temperature interval as in the cooling scan, and its trend in both scans is to shift toward lower temperatures as c increases. But now, after the glass transition, an exothermic peak followed by an endothermic peak shows up, indicating the occurrence of first-order phase transitions of water (crystallization and melting). For water contents from $c = 0.25$ on (Figure 4) the cooling thermograms show one large exothermic peak, whose maximum temperature increases with c. At higher water contents a smaller exothermic peak shows up at higher temperatures; its intensity grows with c, but its temperature remains constant, in contrast to the big exotherm. The glass transition of the hydrogel is in these cooling thermograms no longer visible, but the thermograms indicate a change of baseline from the start to the end of the scan. The heating thermograms corresponding to these compositions exhibit one exothermic followed by two endothermic peaks, the latter one being a small peak located on the shoulder of the bigger endotherm at an invariant temperature. Again, the glass transition of the hydrogel cannot be detected, but a change of baseline from the beginning to the end of the scan is appreciated.

5. Discussion

PEA and PHEA homopolymers have glass transitions temperatures separated some 30 deg (T_g(PEA) ≈ −20 °C and T_g(PHEA) ≈ 10 °C). The occurrence in the $c = 0$ thermogram of a single, broad glass transition at a temperature intermediate to that of both pure homopolymers, $T_{g0} = -10$ °C, is indicative of a good mixing (interpenetration) of both networks. This is probably due to the high degree of cross-linking of both networks, which prevents phase separation during the formation reaction to a greater extent than does a more feeble cross-linking.[5,32] For the same IPN composition, indeed, it has been found that two T_g's are visible in DSC if the cross-linking agent concentration in the monomer solutions is of 1% instead of 2%.[33]

With the temperatures of the different transitions (crystallization and melting of water, hydrogel's glass transition) determined from the cooling and heating thermograms, the temperature−composition diagram in Figure 5 can be drawn. For the hydrogel's glass transition the temperature of the inflection point of the thermogram has been taken, whereas for the phase transitions of water it is the temperature of the maximum of the large exothermal or endothermal peak that is taken. It can be seen that this representation qualitatively corresponds to our discussion held in section 2 (Figure 1). In particular, there is no need to invoke interfacial tension,[12] capillary effects, or confinement (see the references gathered in ref 19) to explain the phase-change temperature depression of water. Indeed, numerical estimates of those effects show them to be much smaller than the temperature depression in question.[19]

Three composition regimes are determined by the experimental water concentrations of $c^{**} = 0.17$ and $c^* = 0.23$. For $0 < c < 0.17$ the system remains homogeneous (no first-order transitions) in both the cooling and the heating scans. This can be proved by the evolution of its T_g, which is that of a homogeneous mixture: for comparison, in Figure 5 the course of T_{gh} predicted by Fox's equation[26]

$$\frac{1}{T_{gh}} = \frac{1-c}{T_{g0}} + \frac{c}{T_{gw}} \tag{1}$$

and by the Couchman−Karasz equation[27]

$$T_{gh} = \frac{(1-c)\Delta c_{p0} T_{g0} + c\Delta c_{pw} T_{gw}}{(1-c)\Delta c_{p0} + c\Delta c_{pw}} \tag{2}$$

is displayed as dotted lines. In eq 2 the values T_{gw}= 134 K and $\Delta c_{pw}(T_g) = 1.94$ J/(g K) are taken from ref 28, and T_{g0}= 263 K and $\Delta c_{p0} = 0.48$ J/(g K) are our experimental values. The good agreement of the data with eq 2 supports the hypothesis of a homogeneous mixture water/polymer as the basic physical picture of the hydrogel. For $0.17 < c < 0.23$ the hydrogel's glass transition is reached on cooling before water can crystallize, $T_c(c) < T_{gh}(c)$; crystallization takes place during the heating scan at temperatures immediately above T_{gh} and is followed by a subsequent melting as the sample reaches T^{**}, as explained in the second section (Figure 1b) of this paper. In Figure 6a this explanation of the

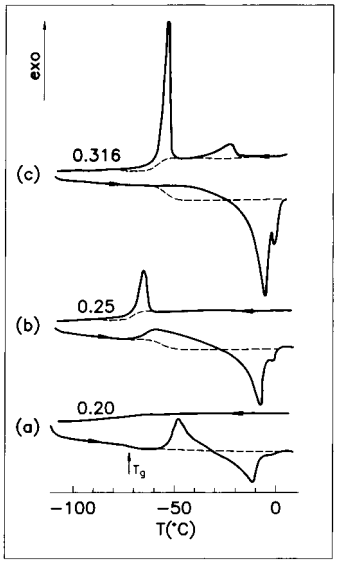

Figure 6. (a) Heating and cooling thermograms of the IPN sample $c = 0.20$. Indicated as a dashed line is the underlying glass transition of the hydrogel. (b) The same for sample $c = 0.25$. (c) The same for sample $c = 0.316$.

two peaks on the heating thermogram is graphically illustrated for the sample $c = 0.20$, where the virtual baseline hidden by the phase transitions of water has been indicated. Moreover, the fact that all water that melts is precisely that which has crystallized during the same heating scan is verified by checking the equality of the crystallization and melting enthalpy increments: for the sample just referred to, these values are, respectively, $\Delta H_c = 233$ mJ and $\Delta H_m = 234$ mJ, as determined by the apparatus software. The same agreement is found for the samples $c = 0.185$ and $c = 0.218$.

For water concentrations greater than 0.23, $T_c(c)$ is reached on cooling before $T_{gh}(c)$. This corresponds to the case $c > c^{**}$ in section 2 (Figure 1c). Water crystallizes upon cooling, originating the exothermic peak in the thermogram. Upon reheating, a further crystallization takes place immediately after $T_{gh}(c)$ has been passed and is followed by the melting of all solid water until $T_m(c)$. Figure 6b illustrates this situation for the sample $c = 0.25$. The hidden virtual baseline has been traced by taking into account the glass transition of the hydrogel. When this is done, the equality of the crystallization and melting heats can be verified:

$$\Delta H_m = \Delta H_c = \Delta H_c(\text{cooling}) + \Delta H_c(\text{heating}) \quad (3)$$

For sample $c = 0.25$, ΔH_c(cooling) = 135 mJ, ΔH_c(heating) = 265 mJ, and $\Delta H_m = 419$ mJ. The slight mismatch is considered to be insignificant and due to the uncertainty in the drawing of the baseline, which must be inferred from the experimental results close to c^* where it is still visible.

For water contents $c = 0.276$, 0.316, and 0.346 a crystallization peak preceeds on cooling the larger exothermic peak just analyzed. The facts that its temperature is very similar to the undercooling lag of pure water and that it shows no dependence on water concentration suggest that it could be due to the crystallization of water present in the sample in some physical state close to that of bulk water, maybe as water aggregates in cavities or pores of the network (water, then, that is not homogeneously mixed with the polymer chains). The growth of this exothermal peak with water concentration is consistent with this explanation. The breadth of the peak, on the other hand, excludes that it could be caused by pure water on the pan released from the sample, which would show a much more narrow profile (Figure 4, curve of water). The existence of such thermal effects associated with bulklike water has been also found in other hydrogels.[9]

When the baseline corresponding to the glass transition of the hydrogel is superposed on the heating thermogram, a broad crystallization peak followed by the melting peak is again revealed; in Figure 6c this is done for the $c = 0.316$ sample. The very weak high-temperature peak on the shoulder of the big endotherm grows larger with increasing c, but its temperature does not depend on c and corresponds to that of the melting of pure water. As already suggested, this peak must be attributed to the melting of a small fraction of water present in the hydrogel in the form of aggregates, probably in larger spaces left by heterogeneities in the network. Again, it is verified that the sum of all crystallization heats equals the melting heat: for the $c = 0.316$ sample,

$$\Delta H_m = \Delta H_c = \Delta H_c^{I}(\text{cooling}) + \Delta H_c^{II}(\text{cooling}) + \Delta H_c(\text{heating}) \quad (4)$$

with ΔH_c^{I}(cooling) = 88 mJ, ΔH_c^{II}(cooling) = 364 mJ, ΔH_c(heating) = 203 mJ, and $\Delta H_m = 634$ mJ.

In contrast to the crystallization and melting peak of pure bulk water, whose breadth extrapolates to zero as the temperature rate tends to zero, the crystallization and melting of the water separated from the hydrogel produce peaks on the thermograms with constant, rate-independent widths, consistent with the explanation pointed out in section 2.

The thermal effects measured during the crystallization and melting events include, besides the corresponding phase transition heats, the heats of demixing and mixing (dilution) of water in the polymer;[14] these are, nevertheless, negligible compared with the phase-change enthalpies. We do not have data for the water/PHEA case, but the data for the system water/PHEMA,[34] which should be comparable to our case, and for other polymers[25] indicate that the enthalpy of mixing is roughly $^1/_{65}$th of that of melting/crystallizing. When the heat of dilution of water in the polymer is neglected, the experimentally measured enthalpy increments associated with the different transitions of water allow an independent determination of the quantities c^*, c^{**}, and thus an independent verification of the model. In particular, ΔH_c(cooling) determines c^*, and the sum ΔH_c(cooling) + ΔH_c(heating) determines c^{**} according to our explanation. Assuming that the specific latent heat of melting of water in the hydrogel is constant and not appreciably different from that of pure water, $\Delta h_{mw} = 334$ J/g, the quantities c^*, c^{**}, and $c_c = c - c^{**}$ (weight fraction of crystallizable water) have been determined for each sample; they are represented in Figure 7. The constancy of the c^* and c^{**} values is a further support of the model here advanced. Numerically, also, the values sensibly agree with those previously inferred from the thermograms to within the uncertainty in the determination of the ΔH's, the influence of simplifying assumptions (constancy of the melting heat of water, neglect of heat of dilution, sharp value of T_{gh}; all water is homogeneously mixed), and experimental error.

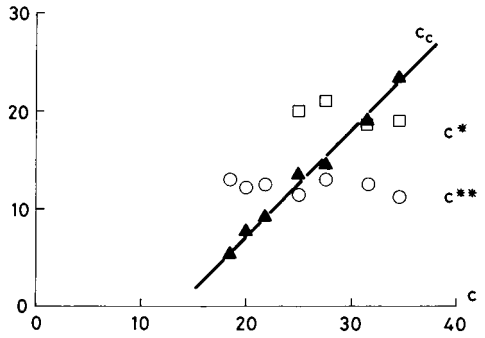

Figure 7. Weight fraction of noncrystallizable water upon cooling c^* (□), of noncrystallizable water upon cooling *and/* heating c^{**} (○), and of crystallizable water c_c (▲), against total weight fraction of water c in the hydrogel, as calculated from the measured enthalpy increments.

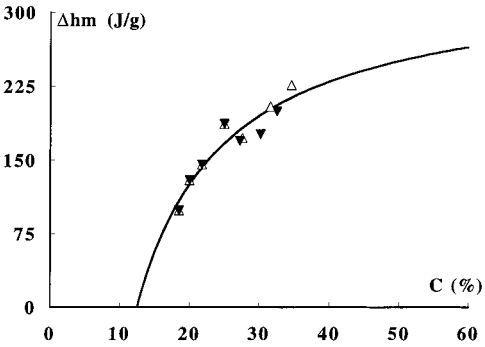

Figure 8. Heat of melting per gram of water *versus/* sample water concentration, as measured (△), and after subtracting from c and Δh_m the contribution of bulklike water (▼). Full line: theoretical curve, eq 5.

The experimentally measured melting heat per gram of water, $\Delta h_m = \Delta H_m/m_w$, has been represented in Figure 8 against the water concentration c in the sample. The dependence of Δh_m on c according to our model is expected to follow the equation

$$\Delta h_m(c) = \left(1 - \frac{c^{**}}{c}\right)\Delta h_{mw} \qquad (5)$$

where, again, the heat of mixing is neglected and Δh_{mw} of pure water is assumed constant. This curve is shown in Figure 8 as a full line, with the value of $c^{**} = 0.125$ determined from the calculations leading to Figure 7.

In Figures 7 and 8 all water is treated as if it were homogeneously mixed with the polymer chains. This is a simplification in so far as the possible existence of some amount of bulklike water in pores or microcavities (heterogeneities of the network) of the hydrogels with higher water contents has been pointed out (see above). The amount of this (nonmixed) bulklike water can be determined in the way just described from the peaks of the thermograms attributed to it, and it can be subtracted from the total amount of water to obtain the quantity of water homogeneously mixed with the polymer chains. This correction has been applied to the data of Figure 8, which shows its negligible effect.

The explanation here advanced of the thermograms in polymeric hydrogels is in line with those authors that have pointed out the effect of the kinetic, nonequilibrium factors affecting the thermal transitions, and in particular, of the hydrogel's glass transition.[14,17] Since it unites equilibrium with nonequilibrium considerations, this scheme is only valid for specified nonequilibrium thermal histories, in our case, those peculiar to scanning calorimetry. Other contexts in which similar pictures based on the state diagram have been proposed include the explanation of crystallization inhibition in blends of semicrystalline and amorphous polymers,[35] and the analysis of hydration and dehydration of biological macromolecules of importance in food processing.[36] Our scheme, in addition, takes into account the further complication introduced by the crystallization and melting temperature depressions and thus is able to explain the most salient feaures observed in DSC thermograms as summarized in refs 9 and 10: the structure of crystallization and melting peaks, the existence of a noncystallizable amount of water (possibly different on cooling and on heating), and the "insensitivity" of DSC to thermal events under a certain temperature.

6. Conclusions

The interpenetrating networks based on the hydrophobic PEA and the hydrophilic PHEA form hydrogels when swollen with water. For a 2% concentration of cross-linking agent the xerogel exhibits a single glass transition, and the hydrogel has an equilibrium water uptake of $c = 0.346$ (swelling ratio $s = 0.530$). The effect of water is to lower the value of the hydrogel's T_g, as would any low molecular weight substance homogeneously mixed with the polymer. The thermal transitions in the hydrogel are governed by the interplay of the glass transition of the (plastified) hydrogel and the phase changes of water. For a given cooling/heating rate, three regimes can be identified according to the water concentration in the hydrogel. In each of them the cooling and heating thermograms show significant differences. The whole phenomenology related to these transitions can be consistently explained on the basis of simple thermodynamic considerations regarding the variations of the glass transition temperature and of the melting and cooling temperatures in binary mixtures. Within this framework, in which no use is made of the hypothesis of different binding strengths of water molecules to polymer chains, these considerations entail the existence of two different (rate-dependent) amounts of "noncrystallizable" water, one for cooling scans, the other for cooling-and-heating scans. Experiment confirms this prediction.

Acknowledgment. Mrs. L. Bueso and Mr. E. Cortés are acknowledged for the preparation of the samples. M.M.P. acknowledges a grant of the Spanish Ministerio de Educación y Ciencia DGICyT PR95-450 for a stay in Orsay while this work was performed and the financial support of project IMPIVA 108994 of the Generalitat Valenciana.

References and Notes

(1) Stoy, V.; Kliment, C. *Hydrogels: Speciality Plastics for Biomedical and Pharmaceutical Applications*; Technomic Publishers: Basel, 1996.
(2) Murayama, S.; Kuroda, S.-I.; Osawa, Z. *Polymer* **1993**, *34*, 2845, 3893.
(3) Eschbach, F. O.; Huang, S. J. In *Interpenetrating Polymer Networks*; Klempner, D., Sperling, L. H., Utracki, L. A., Eds.; Advances in Chemistry Series 239, American Chemical Society: Washington, DC, 1994; Chapter 9.
(4) Ramaraj, B.; Radhakishnan, G. *Polymer* **1994**, *35*, 2167.
(5) Sperling, L. H. *Interpenetrating Polymer Networks and Related Materials*. Plenum Press: New York, London, 1981.
(6) Lipatov, Y. S. In *Interpenetrating Polymer Networks*; Klempner, D., Sperling, L. H., Utracki, L. A., Eds.; Advances in Chemistry Series 239; American Chemical Society: Washington, DC, 1994; Chapter 4.
(7) Corkhill, P. H.; Jolly, A. M.; Ng, C. O.; Tighe, B. J. *Polymer* **1987**, *28*, 1758.

(8) Barnes, A.; Corkhill, P. H.; Tighe, B. J. *Polymer* **1988**, *29*, 2191.
(9) Quinn, F. X.; Kampff, E.; Smyth, G.; McBrierty, V. J. *Macromolecules* **1988**, *21*, 3191.
(10) Smyth, G.; Quinn, F. X.; McBrierty, V. J. *Macromolecules* **1988**, *21*, 3198.
(11) Hofer, K.; Mayer, E.; Johari, G. P. *J. Phys. Chem.* **1990**, *94*, 2689.
(12) Ishikiriyama, K.; Todoki, M. *J. Polym. Sci. B: Polym. Phys.* **1995**, *33*, 791.
(13) Hoeve, C. A. J.; Tate, A. S. *J. Phys. Chem.* **1978**, *82*, 1660.
(14) Pouchlý, J.; Biros, J.; Benes, S. *Makromol. Chem.* **1979**, *180*, 745.
(15) Kyritsis, A.; Pissis, P.; Gómez Ribelles, J. L.; Monleón Pradas, M. *Polym. Gels Networks* **1995**, *3*, 445.
(16) Roorda, W. E.; Bouwstra, J. A.; de Vries, M. A.; Junginger, M. E. *Biomaterials* **1988**, *9*, 494.
(17) Roorda, W. *J. Biomater. Sci. Polym. Ed.* **1994**, *5*, 383.
(18) Rault, J.; Ping, Z. H.; Nguyen, T. *J. Non-Cryst. Solids* **1994**, *172*−174, 733.
(19) Rault, J.; Gref, R.; Ping, Z.; Nguyen, Q. T.; Néel, J. *Polymer* **1995**, *36*, 1655.
(20) Rault, J. *Makromol. Chem., Macromol. Symp.* **1995**, *100*, 31.
(21) Pissis, P.; Kyritsis, A.; Gómez Ribelles, J. L.; Monleón Pradas, M. *J. Polym. Sci. B: Polym. Phys.* **1994**, *32*, 1001.
(22) Pissis, P.; Kyritsis, A.; Gómez Ribelles, J. L.; Monleón Pradas, M. *J. Non-Cryst. Solids* **1994**, *172*−*174*, 1041.
(23) Denbigh, K. *The Principles of Chemical Equilibrium*, 4th ed.; Cambridge University Press: Cambridge, U.K., 1981; Chapter 8.
(24) Flory, P. J. *Principles of Polymer Chemistry*; Cornell University Press: Ithaca, NY, 1971.
(25) Molyneux, P. In *Water. A Comprehensive Treatise*; Franks, F., Ed.; Plenum Press: New York, 1975; Vol. 4.
(26) Fox, T. G. *Bull. Am. Phys. Soc.* **1953**, *1*, 123.
(27) Couchman, P. R. *Macromolecules* **1978**, *11*, 1156.
(28) Johari, G. P.; Hallbrucker, A.; Mayer, E. *Nature* **1987**, *330*, 552.
(29) Becker, R. *Theorie der Wärme*, 3rd ed.; Springer-Verlag: Berlin, New York, *etc.*, 1985; p 60.
(30) Gordon, P. *Principles of Phase Diagrams in Materials Systems*; McGraw Hill: New York, 1968.
(31) Katayama, S.; Fujiwara, S. *J. Phys. Chem.* **1980**, *84*, 2320.
(32) Li, B. Y.; Bi, X. P.; Zhang, D. H.; Wang, F. S. In *Advances in Interpenetrating Polymer Networks*; Klempner, D., Frisch, K. C., Eds.; Technomic Publishers: Lancaster, Basel, 1989; Vol. 1.
(33) Results to be published.
(34) Warren, T. C.; Pims, W. *Macromolecules* **1972**, *5*, 506.
(35) MacKnight, W. J.; Karasz, F. E.; Fried, J. R. In *Polymer Blends*; Paul, D. R., Newman, S., Eds.; Academic Press: San Diego, London, *etc.*, 1978; Vol. 1, Chapter 5.
(36) Slade, L.; Levine, H. *J. Food Eng.* **1994**, *22*, 143.

MA970344I